Spreading and Two-Dimensional Mobility of Long-Chain Alkanes at Solid/Gas Interfaces

Paul Lazar, H. Schollmeyer, and H. Riegler*

Max-Planck-Institut für Kolloid- und Grenzflächenforschung, Am Mühlenberg, D-14476 Potsdam, Germany

(Received 7 April 2004; published 22 March 2005)

Long-chain *n* alkanes on solid surfaces can form partially wetting liquid alkane droplets coexisting with solid multilayer terraces. We propose a diffusivelike alkane flow between terrace edge and droplet perimeter through a molecularly thin "precursorlike" film. Depending on the (uniform!) sample temperature, either droplet or terrace edge are not in thermodynamic equilibrium. This leads to a chemical potential gradient, which drives the reversible alkane flow. The gradient can be adjusted and calculated independently from the phenomenological diffusion coefficient.

DOI: 10.1103/PhysRevLett.94.116101 PACS numbers: 68.08.Bc, 68.43.Jk, 68.55.Ac

Many aspects of wetting, spreading and two-dimensional molecular mobility at solid/gas interfaces are not well understood. Classical thermodynamics and hydrodynamics focus on the macroscopic to mesoscopic scale [1,2]. Statistical thermodynamics and molecular physics describe molecular aspects (e.g., adsorbed films) [3]. Scientific challenges are the crossover from macroscopic to molecular dimensions (e.g., at the droplet perimeter) [2,4] and the spreading kinetics. Theories on spreading focus on a "precursor" film [1,2] supposedly preceding the advancing droplet. Although its existence has already been proven some time ago its properties have been studied experimentally only for a few systems: nematogenic cyanobiphenyls [5], polydimethylsiloxane (PDMS) on silicon wafers [6], and recently Pb/Bi on Cu(111) surfaces [7]. The spreading of PDMS and metal precursors were found ''diffusive'' ($R = \sqrt{D_{app}t}$) in agreement with numerical simulations [8]. The ''apparent'' diffusion coefficient, D_{app}, combines two contributions: a potential gradient and the transport properties of the film [3,9]. In the following we will present experiments on a precursorlike spreading film which allow the adjustment of the driving potential *independent* of the transport properties.

Defined molecularly thin surface coverages of long-chain *n* alkanes (with 15 to 50 C atoms) at SiO_2/air-interfaces are obtained by spin coating of alkane/toluene solutions onto pieces of silicon wafers [10–13], heating the samples above the alkane bulk melting temperatures, T_b, and then cooling them slowly ($\approx 1\,^\circ\mathrm{C}/\mathrm{min}$) to the desired temperature. This heating-cooling cycle ensures reproducible starting conditions.

Well above T_b, an all-liquid, closed alkane film wets the SiO_2 surface. Upon cooling, already a few degrees above T_b, at the "surface freezing temperature," T_{sf}, a wetting transition occurs. Below T_{sf}, liquid bulk alkane droplets partially wet a solid, "surface frozen" alkane monolayer which completely covers the SiO_2 surface. The liquid droplets can be cooled below T_b, without immediate bulk solidification. Instead, for small under-cooling ($\Delta T < 4\,^\circ\mathrm{C}$), the growth of solid monolayer or multilayer terraces coexisting with the liquid bulk droplets can be observed.

As an example the first frame of Fig. 1 [14] shows two droplets at $\Delta T = 1.5\,^\circ\mathrm{C}$ (the contact angle of ≈ 14 deg remains roughly constant during terrace growth). After 30 s, solid terrace rings have grown around the droplets to a width of $\approx 2\ \mu$m, at 96 s to $\approx 4\ \mu$m [15,16]. Between 96 s and 126 s a second terrace grows. The first one does not grow until the second one reaches its edge at 180 s. Thereafter, both grow together.

The terraces consist of multiples of solid monolayers with the molecules standing upright. This can be concluded from (a) uniform and discrete brightness values in the optical microscopy, (b) Brewster angle microscopy data, (c) the height of the terrace edges measured by atomic force microscopy [17], and (d) x-ray reflectivity and diffraction data.

Figure 2 presents monolayer terrace growth kinetics of $C_{30}H_{62}$ and $C_{36}H_{74}$ at $3.0\,^\circ\mathrm{C}$ undercooling. There are differences in the slopes, D_{app}, but all growths can universally be linearized with the squared difference between the

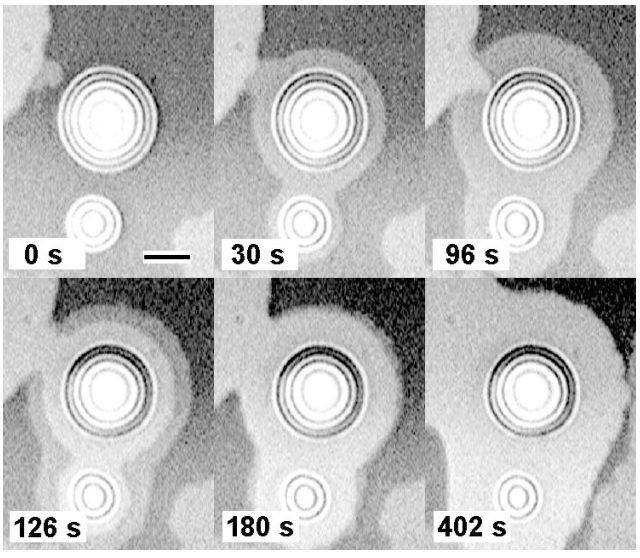

FIG. 1. Growth of alkane monolayer and bilayer terraces (optical reflection microscopy, $C_{36}H_{74}$, $1.5\,^\circ\mathrm{C}$ undercooling, bar = 5 μm).

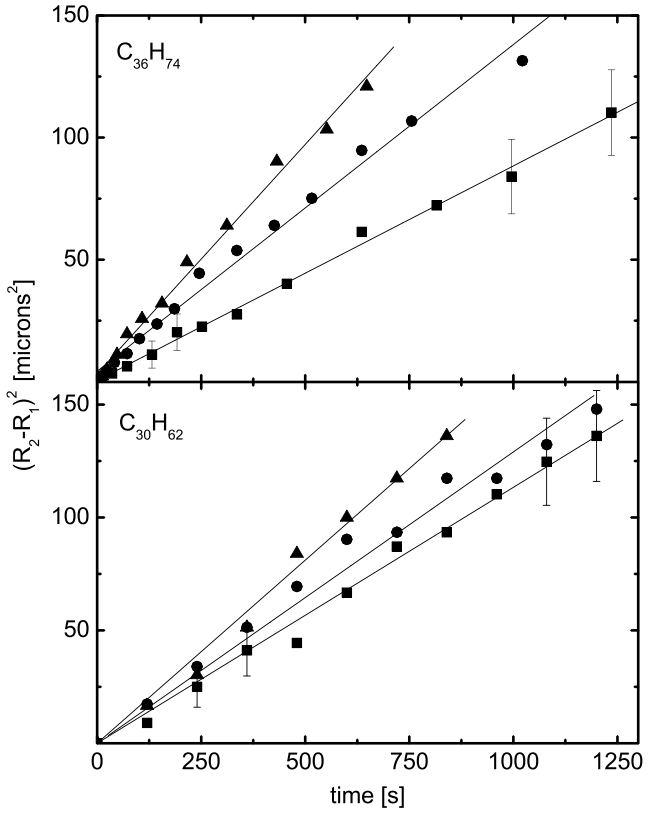

FIG. 2. Growth kinetics of monolayer terraces (3.0 °C undercooling, for the definition of R_1 and R_2 see Fig. 5).

terrace edge radius, R_2, and the drop perimeter, R_1, respectively, as a function of time: $(R_2 - R_1)^2 = D_{\mathrm{app}}t$.

Figure 3 presents the analysis of a sequential growth of two terraces on top of each other. The first monolayer grows with $D^1{}_{\mathrm{app}}(\approx 0.075\ \mu\mathrm{m}^2/\mathrm{s})$ up to t_1. It stops growing as soon as the second plateau starts to grow at similar speed ($D^2{}_{\mathrm{app}} = 0.076\ \mu\mathrm{m}^2/\mathrm{s}$). At t_2 the second plateau reaches the edge of the first one. Then both grow together at about half the speed ($D^{12}{}_{\mathrm{app}} \approx 0.038\ \mu\mathrm{m}^2/\mathrm{s}$).

Figure 4 shows the temperature behavior of D_{app} for three series of growth experiments from the same sample area at different undercooling (random undercooling sequence to reduce systematic errors). Although there are variations, for all samples, D_{app} decreases linearly with decreasing undercooling and the curves can be extrapolated through the origin at T_b.

We propose that the liquid alkane droplets partially wet the circular, solid monolayer-multilayer terraces (see Fig. 5, for simplicity only depicting a monolayer). Droplets and terraces are placed on the solid (''frozen'') alkane monolayer which completely covers the planar SiO_2 substrate. We assume an alkane flow between terrace edges and droplet perimeters through thin alkane films on top of the terraces (''film'' denotes a coverage with mobile alkanes, ''layer'' always refers to a lamella of solid alkane). Most likely this film is not intercalated between the terrace layers if the alkane droplets partially wet the top of continuous terraces as shown in Fig. 5 [18]. The molecules would have to cross the solid monolayer(s). However if the droplets contact directly the frozen monolayer or the substrate, we cannot exclude that the alkanes may flow through a film intercalated between the SiO_2 surface and the frozen solid monolayer (ellipsometric data indicate such a topography [13]). Furthermore, besides the film on the terraces we also propose a film on top of the frozen monolayer as a result of the observations presented in Fig. 6.

For our theoretical description of the terrace growth we assume alkane conservation. The alkane vapor pressure is very low. Small droplets shrink while the terrace(s) grow and the terrace growth stops when they disappear. Also, if the terrace shrinks, small droplets grow (Fig. 6). We further assume isolated droplets without alkane exchange between neighboring droplets and terraces.

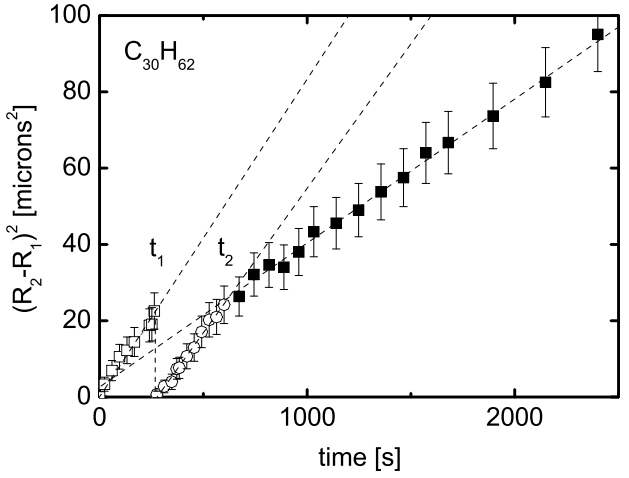

FIG. 3. Growth kinetics of a monolayer terrace followed by a second monolayer terrace on top, $C_{30}H_{62}$, 2.0 °C undercooling.

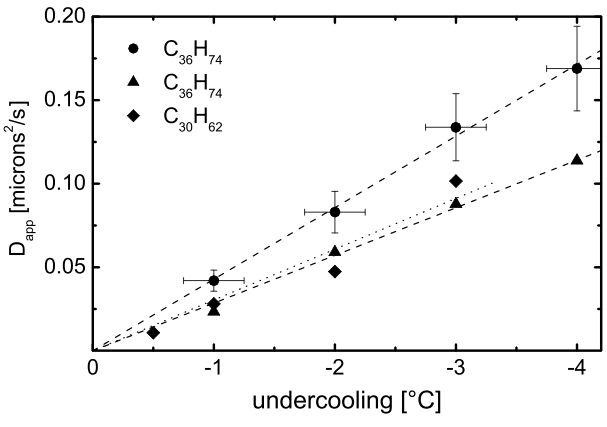

FIG. 4. Temperature behavior of D_{app} for three series of experiments (for each series: same area and preparation history, random variation of the undercooling).

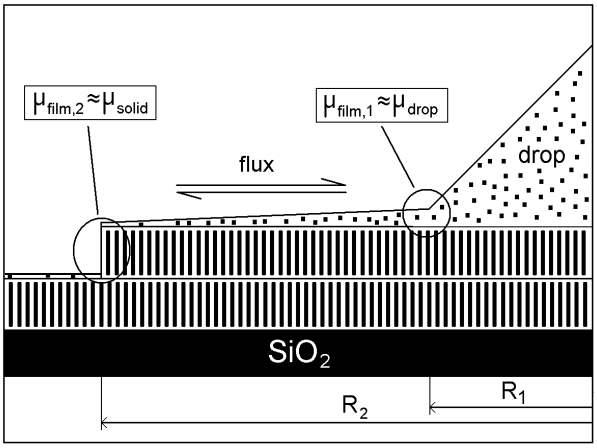

FIG. 5. Proposed topology and scenario of the spreading and terrace growth.

Accordingly, the experimental data presented in Figs. 2–4 were derived from terrace perimeter sections much closer to their ''own'' droplets than to neighboring terrace edges (any ''external'' supply from nearby droplets or terraces can be identified through a growing bulge in the terrace perimeter, see Fig. 1). We predict a diffusive transport between the droplet perimeter and the terrace edge. In general terms, the diffusive flux is $j = -L\nabla\mu$ (L = phenomenological diffusion coefficient, $\nabla\mu$ = the potential gradient). In our case the flux is driven by a potential gradient in the film between droplet and terrace edge. At its boundaries, the film shall have the potential of the bulk droplet (μ_{drop}) and of the solid terrace edges (μ_{solid}). This causes a potential difference because either droplet (for $T < T_b$) or terrace edge (for $T > T_b$) are not in thermodynamic equilibrium, i.e., $\mu_{\text{solid}} \neq \mu_{\text{drop}}$ (except for $T = T_b$, please note: there is *no* thermal gradient; the sample is at uniform temperature). This generates a gradient $\nabla\mu = \Delta\mu/(R_2 - R_1) = (\mu_{\text{solid}} - \mu_{\text{drop}})/(R_2 - R_1)$, which after the integration of $j = -L\nabla\mu$ leads to (ρ = number of moles of solid alkane per terrace area).

$$\frac{R_2^2}{2}\left(2\ln\frac{R_2}{R_1} - 1\right) + \frac{R_1^2}{2} \overset{\frac{R_2}{R_1}\Rightarrow 1}{\approx} (R_2 - R_1)^2 = -\frac{2L\Delta\mu}{\rho}t \overset{!}{=} D_{\text{app}}t$$

This agrees with the observed terrace growth [19,20]. It also explains the increase of the terrace growth speed with decreasing temperature via $\Delta\mu \approx S_m\Delta T$ (S_m = molar entropy of fusion, and $\Delta T = T - T_b$). As $\Delta\mu$ can be positive or negative for $T > T_b$ or $T < T_b$, respectively, this result predicts that the alkane flow might be reversible. This it is indeed, which is quite unique and validates our model. The terraces can be heated slightly above the bulk melting point (at most by $\approx 0.3\,^\circ$C) without melting them macroscopically. The terrace perimeter shrinks as the molecules flow "back" from the terrace edge to the droplet. Alternatively, quite often, a groove appears in the terrace (its bottom is the frozen monolayer surface) at the droplet perimeter and widens (Fig. 6). In the first frame one can see a big and a small droplet surrounded by terrace areas. A lengthy trench in the terrace area extends from the upper left corner. This trench grows and eventually leads to a groove around the large droplet which widens in time with a diffusive exponent of ≈ 0.5. The alkanes migrate over the frozen monolayer towards the droplet. This proves the existence of the precursorlike film also on the surface frozen monolayer (not unexpected due to its structural similarity to terrace surfaces).

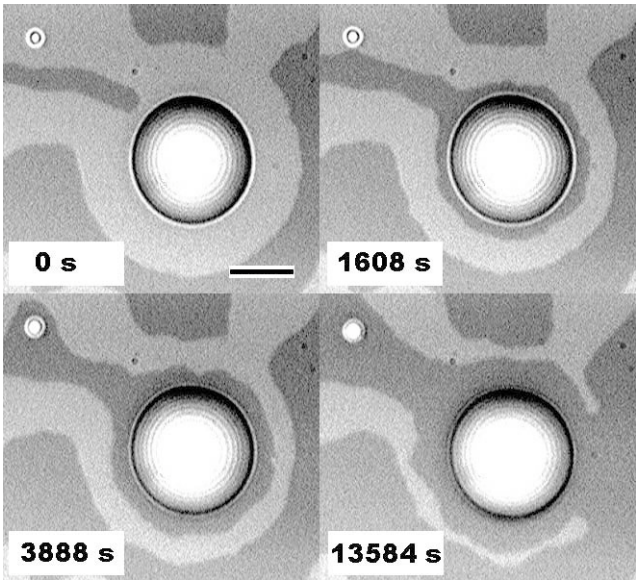

FIG. 6. Gradual elimination of the monolayer terrace (brighter area) due to an alkane flux towards the droplets ($\approx 0.3\,^\circ$C above bulk melting, $C_{30}H_{62}$, bar = 10 μm).

In conclusion, 2-dimensional transport and wetting phenomena were studied with molecularly thin coverages of long-chain alkanes on solid surfaces. In the vicinity of the bulk melting temperature partially wetting alkane droplets are surrounded by a ''precursorlike'' molecularly thin film of mobile alkanes. For temperatures below bulk melting a diffusive alkane transport through this film supplies the growth of solid multilayer terraces surrounding the (undercooled) liquid droplets. For temperatures above bulk melting the alkane flux can be reversed, the solid terraces shrink. The flux is driven by the chemical potential difference between droplet and terrace edge with one or the other not in thermodynamic equilibrium (the sample is at uniform temperature). The unique experimental configuration permits the independent adjustment and derivation of the driving potential and of the surface transport properties, respectively, ($L \approx 6E - 22[\text{mol}^2/(\text{s Nm})]$, assuming bulk values for S_m).

Discussions with H. Möhwald, R. Köhler, and Daniel Rapoport are gratefully acknowledged. P. L. was supported by the International Max Planck Research School on Biomimetic Systems.

*Electronic address: Hans.Riegler@mpikg.mpg.de

[1] A. Marmur, Adv. Colloid Interface Sci. **19**, 75 (1983).
[2] P. G. de Gennes, Rev. Mod. Phys. **57**, 827 (1985).
[3] R. Gomer, Rep. Prog. Phys. **53**, 917 (1990).
[4] J. F. Joanny and P. G. de Gennes, J. Phys. (Paris) **47**, 121 (1986); G. J. Hirasaki, in *Contact Angle, Wettability and Adhesion*, edited by K. L. Mittal (VSP International Science Publishers, Leiden, The Netherlands, 1993), p. 183; L. M. Pismen and Y. Pomeau, Phys. Rev. E **62**, 2480 (2000).
[5] J. Daillant *et al.*, Phys. Rev. A **46**, R6158 (1992); O. Ou Ramdane *et al.*, Phys. Rev. Lett. **80**, 5141 (1998); F. Vandenbrouck *et al.*, Phys. Rev. Lett. **81**, 610 (1998); S. Betelu *et al.*, Phys. Rev. E **59**, 6699 (1999); L. Xu *et al.*, Phys. Rev. Lett. **84**, 1519 (2000); R. Lucht and C. Bahr, Phys. Rev. Lett. **85**, 4080 (2000); D. van Effenterre *et al.*, Phys. Rev. Lett. **87**, 125701 (2001).
[6] D. Ausserré *et al.*, Phys. Rev. Lett. **57**, 2671 (1986); L. Léger *et al.*, Phys. Rev. Lett. **60**, 2390 (1988); F. Heslot *et al.*, Phys. Rev. Lett. **62**, 1286 (1989); A. M. Cazabat *et al.*, Phys. Rev. E **49**, 4149 (1994); M. P. Valignat *et al.*, Phys. Rev. Lett. **80**, 5377 (1998).
[7] J. Moon *et al.*, Langmuir **20**, 402 (2004).
[8] J. De Coninck *et al.*, Phys. Rev. E **48**, 4549 (1993); J. De Coninck *et al.*, Langmuir **9**, 1906 (1993); J. De Coninck *et al.*, Phys. Rev. Lett. **74**, 928 (1995); S. Bekink *et al.*, Phys. Rev. Lett. **76**, 3766 (1996); S. F. Burlatsky *et al.*, Phys. Rev. E **54**, 3832 (1996); G. Oshanin *et al.*, Phys. Rev. E **58**, R20 (1998); D. B. Abraham *et al.*, Phys. Rev. Lett. **88**, 206101 (2002).
[9] T. Ala-Nissila *et al.*, Phys. Rev. Lett. **76**, 4003 (1996); T. Hjelt *et al.*, Phys. Rev. E **57**, 1864 (1998); S. A. Sukhishvili *et al.*, Nature (London) **406**, 146 (2000); T. Hjelt and I. Vattulainen, J. Chem. Phys. **112**, 4731 (2000); P. Nikunen *et al.*, J. Chem. Phys. **114**, 6335 (2001).
[10] The wafers had artificially grown thick oxide layers ($\approx$300 nm) for higher imaging contrast. The wetting properties are largely identical to the naturally oxidized surfaces investigated previously [11,12].
[11] C. Merkl *et al.*, Phys. Rev. Lett. **79**, 4625 (1997).
[12] A. Holzwarth *et al.*, Europhys. Lett. **52**, 653 (2000); H. Schollmeyer *et al.*, Langmuir **18**, 4351 (2002); H. Schollmeyer *et al.*, Langmuir **19**, 5042 (2003).
[13] U. G. Volkmann *et al.*, J. Chem. Phys. **116**, 2107 (2002); H. Mo *et al.*, Chem. Phys. Lett. **377**, 99 (2003).
[14] See EPAPS Document No. E-PRLTAO-94-002514 for a time-lapsed movie (c36_ind43sSCL.avi) showing the terrace growth from another experiment. A direct link to this document may be found in the online article's HTML reference section. The document may also be reached via the EPAPS homepage (http://www.aip.org/pubserves/epaps.html) or from ftp.aip.org in the directory /epaps/. See the EPAPS homepage for more information.
[15] For isolated droplets the nucleation of the terrace growth is a rare event. For sufficient droplet density "secondary nucleation" is dominating: a growing terrace front (e.g., in Fig. 1 from the upper left corner) touches the perimeter of a droplet without terrace and triggers the terrace growth. Thus, a single, rare terrace growth event initiates widespread and easily observable terrace growth.
[16] See EPAPS Document No. E-PRLTAO-94-002514 for terrace nucleation from an isolated droplet on SingleDrop.pdf. A direct link to this document may be found in the online article's HTML reference section. The document may also be reached via the EPAPS homepage (http://www.aip.org/pubserves/epaps.html) or from ftp.aip.org in the directory /epaps/. See the EPAPS homepage for more information.
[17] See EPAPS Document No. E-PRLTAO-94-002514, Terrace_Steps_C36-1.pdf. A direct link to this document may be found in the online article's HTML reference section. The document may also be reached via the EPAPS homepage (http://www.aip.org/pubserves/epaps.html) or from ftp.aip.org in the directory /epaps/. See the EPAPS homepage for more information.
[18] Figure 5 shows only the most plausible droplet positioning, i.e., on top of the solid alkane layers.
[19] If the spreading kinetics were only release- or growth-limited, the circular geometry alone would lead to a square-root time behavior of the radii, with $R_2^2 - R_1^2 \propto t$. This, however, is clearly different from a diffusionlike flux proportional to $\nabla\mu$ between R_1 and R_2, with $(R_2 - R_1)^2 \propto t$ for R_2 close to R_1 (i.e., in the early stages of the spreading). The observed data can only be linearized with the latter; the deviations to the differences of the squares are quite evident. The spreading is definitely ''diffusive.''
[20] For a comparison of the two behaviors $R_2^2 - R_1^2 \propto t$ and $(R_2 - R_1)^2 \propto t$, respectively, see EPAPS Document No. E-PRLTAO-94-002514, Sqrt2.pdf. A direct link to this document may be found in the online article's HTML reference section. The document may also be reached via the EPAPS homepage (http://www.aip.org/pubserves/epaps.html) or from ftp.aip.org in the directory /epaps/. See the EPAPS homepage for more information.